Epitaxial two-dimensional nitrogen atomic sheet in GaAs

Harada, Yukihiro
Yamamoto, Masuki
Baba, Takeshi
Kita, Takashi

(Citation)
Applied Physics Letters,104:041907-041907

(Issue Date)
2014

(Resource Type)
journal article

(Version)
Version of Record

(URL)
https://hdl.handle.net/20.500.14094/90002576

Epitaxial two-dimensional nitrogen atomic sheet in GaAs

Yukihiro Harada, Masuki Yamamoto, Takeshi Baba, and Takashi Kita

Citation: Applied Physics Letters **104**, 041907 (2014); doi: 10.1063/1.4863442
View online: http://dx.doi.org/10.1063/1.4863442
View Table of Contents: http://scitation.aip.org/content/aip/journal/apl/104/4?ver=pdfcov
Published by the AIP Publishing

Epitaxial two-dimensional nitrogen atomic sheet in GaAs

Yukihiro Harada,[a] Masuki Yamamoto, Takeshi Baba, and Takashi Kita
Department of Electrical and Electronic Engineering, Graduate School of Engineering, Kobe University, 1-1 Rokkodai, Nada, Kobe 657-8501, Japan

(Received 21 December 2013; accepted 13 January 2014; published online 29 January 2014)

We have grown an epitaxial two-dimensional nitrogen (N) atomic sheet in GaAs by using the site-controlled N δ-doping technique. We observed a change of the electronic states in N δ-doped GaAs from the isolated impurity centers to the delocalized impurity band at 1.49 eV with increasing N-doping density. According to the excitation-power- and temperature-dependent photoluminescence (PL) spectra, the emission related to localized levels below the impurity band edge was dominant at low excitation power and temperature, whereas the effects of the localized levels can be neglected by increasing the excitation power and temperature. Furthermore, a clear Landau shift of the PL-peak energy was observed at several Tesla in the Faraday configuration, in contrast to the case in the impurity limit. © *2014 AIP Publishing LLC*. [http://dx.doi.org/10.1063/1.4863442]

Single-layer atomic sheets, such as graphene,[1,2] silicene,[3,4] and germanane,[5] have attracted considerable interest over the past decade as ideal two-dimensional systems since the successful isolation of graphene sheets.[6] One of the most interesting aspects of single-layer atomic sheets arranged in a regular hexagonal pattern is their massless, chiral Dirac fermions.[7] A promising application of single-layer atomic sheets is in field-effect-transistor channels because these sheets have extremely high carrier mobility. The carrier mobility of single-layer graphene is as high as 1 000 000 $cm^2/V{\cdot}s$ at 2 K (Ref. 8) and 200 000 $cm^2/V{\cdot}s$ at room temperature.[9] However, their gapless band structure requires bilayer,[10] nanoribbon,[11] or nanomesh[12] structures to open the band gap for achieving a large on/off current ratio. According to theoretical calculations based on a tight-binding approach, graphene nanoribbons and nanomeshes have a band-gap energy and effective mass on the order of 1 eV and $0.1m_0$, respectively,[13] where m_0 is the electron rest mass. Conversely, engineering a graphene band gap reduces the carrier mobility.[14] An embedded channel in the host matrix, rather than an isolated one, is preferred for practical applications.

Recently, single impurity centers or dopants in semiconductors have been considered as qubits for quantum computing and nonclassical light sources for quantum information processing as well as quantum dots (QDs) (see, for example, Refs. 15 and 16, and references therein). The electronic state of the localized impurity level is uniquely determined by a combination of the host matrix and the impurity centers. Therefore, coherently coupled electronic states among the impurities are expected for highly impurity-doped semiconductors in an atomically controlled manner. This is in contrast to the case of self-organized QDs because the inhomogeneous distribution of the size and shape of the QDs prevent the formation of coherently coupled electronic states in the growth plane.

In this Letter, we report on the control of electronic states of a nitrogen (N) atomic sheet embedded in a GaAs host matrix fabricated using the site-controlled N δ-doping technique.[17] The uniform N-pair centers, formed in an atomically controlled manner, act as an isoelectronic trap in the impurity limit, which is regarded as an ideal QD.[17–19] Conversely, a change of their electronic states from the isolated impurity centers to the delocalized impurity band at 1.49 eV has been observed with increasing N-doping density. Furthermore, the photoluminescence (PL)-peak energy of the 1.49-eV line in highly N δ-doped GaAs showed a clear Landau shift at several Tesla (T) in the Faraday configuration, which implies the magnetic quantization of the delocalized energy states in the growth plane. The effective mass of the optically excited carrier was estimated using the Landau shift as approximately $0.07m_0$.

The samples were grown by molecular beam epitaxy on GaAs-buffer layers on semi-insulating GaAs(001) substrates. Before N doping, a 300-nm-thick $Al_{0.3}Ga_{0.7}As$ and 50-nm-thick GaAs layers were grown at 550 °C with an As_2 flux of 1.3×10^{-3} Pa. The N doping was performed on the $(2 \times 4)\beta 2$ surface at 550 °C with an As_2 flux of 4.0×10^{-4} Pa and nitridation durations of 100, 300, and 1000 s achieved using active N species created in a radio-frequency plasma source from ultrapure N_2 gas. The gas-flow rate was 0.37 ccm. After a growth interruption of 120 s, a 50-nm-thick GaAs layer was grown at 550 °C with an As_2 flux of 4.0×10^{-4} Pa. Subsequently, a 100-nm-thick $Al_{0.3}Ga_{0.7}As$ and 10-nm-thick GaAs-capping layers were grown at 550 °C with an As_2 flux of 1.3×10^{-3} Pa. The 100-nm-thick active layer of GaAs:N was sandwiched between $Al_{0.3}Ga_{0.7}As$ barrier layers to achieve efficient carrier capture in the active layer.[20] According to secondary ion-microprobe mass spectrometry, the N sheet densities were approximately 5×10^2, 1×10^3, and 4×10^3 μm^{-2} for the samples with nitridation durations of 100, 300, and 1000 s, respectively.

PL measurements were performed using a continuous-wave laser beam with a wavelength of 484 nm. The samples were mounted in a superconducting-magnet system cooled by a He-gas flow for the magneto-PL measurement, and in a closed-cycle cryostat for the other measurements. The PL was dispersed in a monochromator and detected using a liquid-N_2-cooled Si charge-coupled device array. An 85-cm double monochromator was used for the magneto-PL

[a]Electronic mail: y.harada@eedept.kobe-u.ac.jp

measurement, and a 55-cm single monochromator was used for the other measurements. The spectrum resolutions of our spectroscopy system with the double and single monochromators were approximately 35 and 150 μeV, respectively. A magnetic field was applied in the [001] direction in the Faraday configuration.

Figure 1(a) shows typical PL spectra of N δ-doped GaAs grown with different N-sheet densities at 3.1 K. The bottom, middle, and top spectra are the results for samples with N sheet densities, $[N]_{2D}$, of approximately 5×10^2, 1×10^3, and 4×10^3 μm^{-2}, respectively. The excitation power was 0.1 mW. The PL intensities were normalized by those of the 1.493-eV line. The sharp emission lines observed at 1.444 and 1.493 eV are attributed to the excitons bound to the first- and fourth-nearest neighbor N pairs on the (001) plane, respectively.[19] The PL signal of the 1.444-eV line becomes significant with an increase in the N sheet density. This indicates that the density of the first-nearest-neighbor N-pair centers becomes greater than that of the fourth-nearest-neighbor N-pair centers. The sharp emission lines arising from the pairs on the (001) plane[17–19] indicate that almost all N-pair centers are formed on the (001) growth plane.[21] Therefore, coherently coupled electronic states among the N-pair centers in the growth plane are expected in the highly N δ-doped GaAs. It is worth noting that a broad PL band with a full width at half maximum of 9 meV appeared at 1.49 eV for the sample with an $[N]_{2D}$ of 4×10^3 μm^{-2}, which indicates interaction among the fourth--nearest-neighbor N pairs. In other words, the broad PL band indicates a change of their electronic states from the isolated impurity centers to the delocalized impurity band with increasing N-doping density. Conversely, an $[N]_{2D}$ of 4×10^3 μm^{-2} corresponds to a fourth-nearest-neighbor N-pair density of less than 10 μm^{-2}.[22] Since the Bohr radius of the exciton bound to the fourth-nearest-neighbor N pair is less than 5 nm,[19] the N-pair density of less than 10 μm^{-2} is too low to induce the interaction between the N-pair centers. Therefore, the observed broad PL band reflecting the interaction among the fourth-nearest-neighbor N pairs suggests that a sort of aggregation of N-pair centers is inhomogeneously formed in the (001) growth plane. Excitation power dependences of the integrated PL intensity for the 1.49-eV line are shown in Figs. 1(b)–1(d) for $[N]_{2D}$ values of 5×10^2, 1×10^3, and 4×10^3 μm^{-2}, respectively. The integrated PL intensities were saturated for the samples with $[N]_{2D} = 5 \times 10^2$ and 1×10^3 μm^{-2}, whereas it linearly increased with the increase in the excitation power for the sample with an $[N]_{2D}$ of 4×10^3 μm^{-2}. This result suggests that the density of state of the 1.49-eV line became large for this sample. Figure 1(e) shows the excitation power dependence of the PL spectrum for the sample with an $[N]_{2D}$ of 4×10^3 μm^{-2}. The PL intensities were normalized by those of the 1.49-eV line. The PL intensity of the 1.444-eV line tended to saturate with an increase in excitation power, whereas that of the 1.49-eV line linearly increased as shown in Fig. 1(d). This result clearly indicates that the density of state of the 1.49-eV line is larger than that of the 1.444-eV line owing to the first-nearest-neighbor N-pair centers. This is due to the formation of the impurity band of the 1.49-eV line. The PL peak energy of the 1.49-eV line showed a blue shift of approximately 2.3 meV with an increase in excitation power. Conversely, the PL spectrum becomes asymmetric when excited below the excitation power of 0.1 mW. Similar asymmetric PL spectra have been observed in GaInNAs alloys as a result of the localized levels below the conduction band.[23,24] Therefore, the excitation-power dependent PL spectra in Fig. 1(e) suggests the existence of the localized level below the impurity band edge.

To confirm the effect of the carrier localization, we performed temperature-dependent PL measurements. Figure 2(a) shows the temperature dependence of the PL spectra for the sample with an $[N]_{2D}$ of 4×10^3 μm^{-2}. The excitation power was 10 mW. The PL intensities were normalized by those of the 1.49-eV line. The PL intensity of the 1.49-eV line significantly decreased when the temperature was increased, and that of the 1.51-eV line became dominant. Similar temperature-dependent PL spectra in GaInNAs quantum wells are explained by the presence of N-induced localized states.[25,26] Therefore, these changes of the dominant PL lines in Fig. 2(a) suggest that an aggregation of N-pair centers is inhomogeneously formed in the (001) growth plane as discussed in Fig. 1(a); the N-pair centers both with and without interaction among the N pairs exist in the growth plane. The complex structure of the 1.51-eV line indicates the

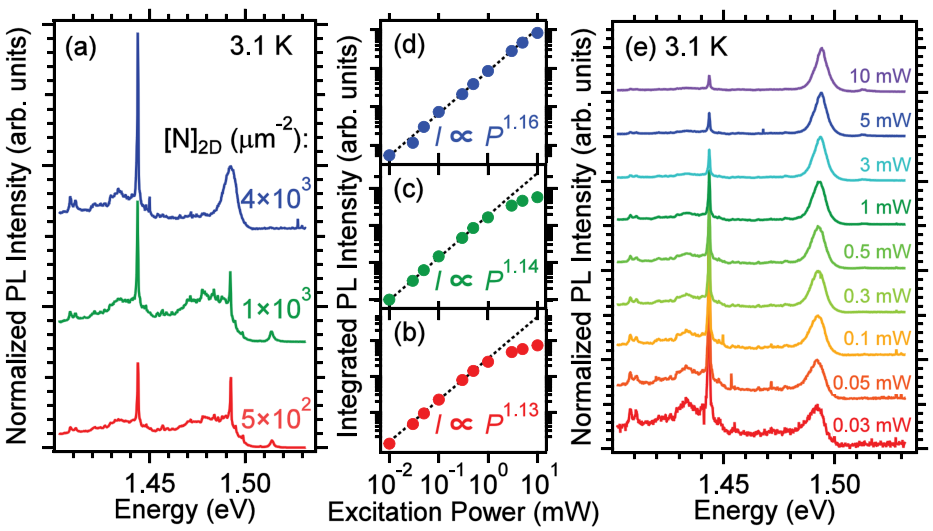

FIG. 1. (a) Typical PL spectra of N δ-doped GaAs grown with different N-sheet densities at 3.1 K. The excitation power was 0.1 mW. The PL intensities were normalized by those of the 1.493-eV line. (b)–(d) Excitation power dependencies of the integrated PL intensity of the 1.49-eV line for the samples with $[N]_{2D}$ values of 5×10^2, 1×10^3, and 4×10^3 μm^{-2}, respectively. (e) Excitation power dependence of the PL spectrum for the sample with an $[N]_{2D}$ of 4×10^3 μm^{-2}. The PL intensities were normalized by those of the 1.49-eV line.

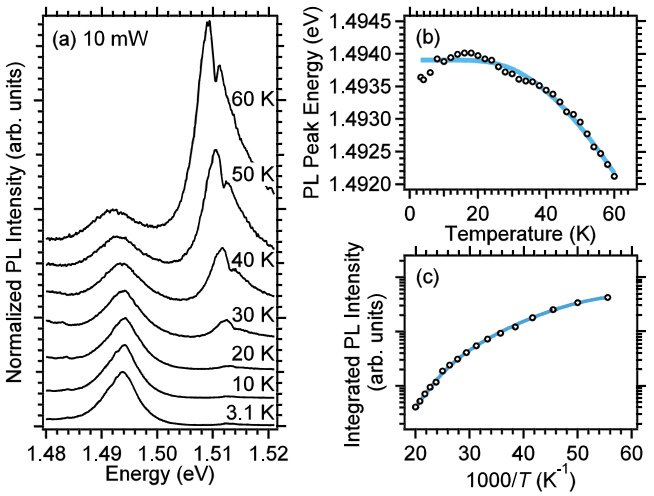

FIG. 2. (a) Temperature dependence of the PL spectra for the sample with an $[N]_{2D}$ of $4 \times 10^3\ \mu m^{-2}$. The excitation power was 10 mW. The PL intensities were normalized by those of the 1.49-eV line. Temperature dependence of (b) the PL peak energy and (c) the integrated PL intensity of the 1.49-eV line. The solid lines in (b) and (c) are the fitting curves obtained by considering a Bose-Einstein type formula and a two-channel Arrhenius formula, respectively.

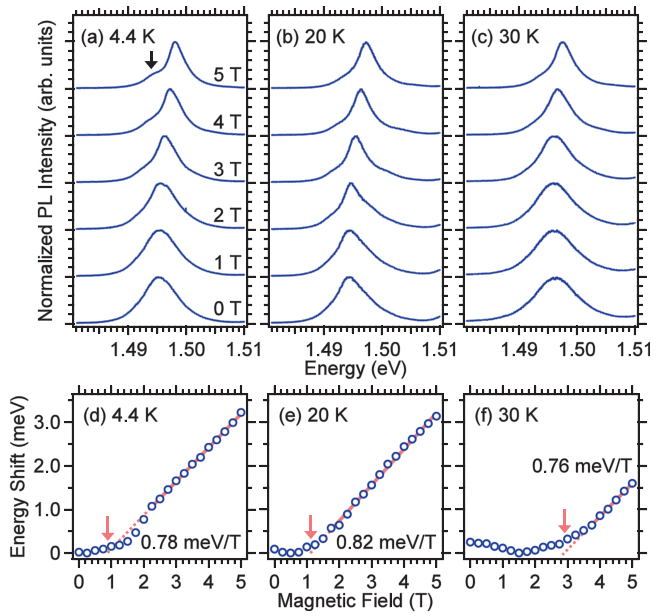

FIG. 3. Normalized magneto-PL spectra at (a) 4.4, (b) 20, and (c) 30 K, respectively, for the sample with an $[N]_{2D}$ of $4 \times 10^3\ \mu m^{-2}$. The excitation density was $9.3\ W/cm^2$, which corresponds to the excitation power of ~1 mW in Fig. 1. (d)–(f) Magnetic field dependence of the PL-peak energy at each temperature. The minimum PL-peak energy at each temperature was set to zero. The solid lines indicate the linear magnetic-field dependence.

interaction between the conduction-band edge and N-related localized levels observed in the N δ-doped GaAs in the impurity limit.[27] Figure 2(b) shows the temperature dependence of the PL-peak energy of the 1.49-eV line. The PL-peak energy showed a blue shift with an increase in temperature up to 18 K. This result indicates that the emission related to localized levels was dominant below 18 K as discussed in Fig. 1(e). Conversely, the PL-peak energy showed a red shift with an increase in the temperature above 18 K. The solid line in Fig. 2(b) indicates a fitting curve obtained by considering a formula of Bose-Einstein type:[28,29] $E_g(T) = E_g(0) - S\langle\hbar\omega\rangle[\coth(\langle\hbar\omega\rangle/2k_BT) - 1]\rangle$, where k_B is the Boltzmann constant, E_g (0) is the band-gap energy at zero Kelvin, S is a dimensionless coupling constant, and $\langle\hbar\omega\rangle$ is the average phonon energy. The obtained parameters E_g (0), S, and $\langle\hbar\omega\rangle$ were 1.4939 eV, 0.721 ± 0.104, and 12.6 ± 1.0 meV, respectively. Figure 2(c) shows the temperature dependence of the integrated PL intensity of the 1.49-eV line. We estimated the thermal quenching activation energies above 18 K, where the effect of the localized levels can be neglected. By using a two-channel Arrhenius formula, the activation energies were estimated to be 11.3 ± 6.7 and 36.4 ± 0.2 meV. These activation energies are comparable to the average phonon energy obtained in Fig. 2(b) and longitudinal-optical phonon energy of 35.3 meV in GaAs.[30]

Magneto-PL measurements were performed to evaluate the carrier localization from another viewpoint. Figures 3(a)–3(c) show normalized magneto-PL spectra in the Faraday configuration at 4.4, 20, and 30 K, respectively, for the sample with an $[N]_{2D}$ of $4 \times 10^3\ \mu m^{-2}$. The excitation density was $9.3\ W/cm^2$, which corresponds to the excitation power of ~1 mW in Fig. 1. From the bottom, the magnitude of magnetic field is increased from 0 to 5 T. The PL-peak energy shows a clear blue shift with an increase in the magnetic field at all temperatures. Figures 3(d)–3(f) show the magnetic field dependence of the PL-peak energy at each temperature. Here, the minimum PL-peak energy at each temperature was set to zero. At 4.4 K, the PL-peak energy showed a quadratic shift of $0.11\ meV/T^2$ below 1.5 T, which indicates that the magnetic field can be treated as a perturbation for the exciton in highly N δ-doped GaAs only below 1.5 T. The quadratic shift of $0.11\ meV/T^2$ is several tens of times larger than that in the impurity limit.[19] Conversely, the PL-peak energy showed a clear linear shift of 0.78 meV/T above 2.5 T. The linear shift (Landau shift) implies the magnetic quantization of the delocalized energy states in the growth plane. This result is in contrast to the case in the impurity limit that the magnetic field is regarded as a perturbation at least up to 5 T.[19] These results imply that the electronic states delocalize in the growth plane in highly N δ-doped GaAs. According to $\Delta E = (e\hbar/2\mu)B$, the in-plane reduced effective mass of the exciton, μ, was estimated to be $0.074m_0$. The linear shifts of 0.82 and 0.76 meV/T at 20 and 30 K in Figs. 3(e) and 3(f) correspond to the effective masses of $0.071m_0$ and $0.076m_0$, respectively. Since the N atoms are considered to act as electron traps, these reduced masses would be consistent with hole masses.[31] On the other hand, at 4.4 K, another PL peak appeared in the low energy side at magnetic fields above 4 T, as depicted by an arrow in Fig. 3(a). This PL peak in the low energy side results from the uncoupled, localized level below the impurity band edge as discussed in the temperature and excitation power dependences of the PL spectra. Furthermore, at 30 K, the PL-peak energy shows a red shift below 1.5 T, as shown in Fig. 3(f). These features indicate the competition between the carrier delocalization by the thermal energy and carrier localization by the magnetic field.

The cyclotron angular frequency ω_c is represented by eB/μ, and the Landau shift can be observed when $\hbar\omega_c > k_BT$ and $\omega_c\tau > 1$, where τ is the carrier relaxation time. Therefore, an upper limit of the temperature and a lower

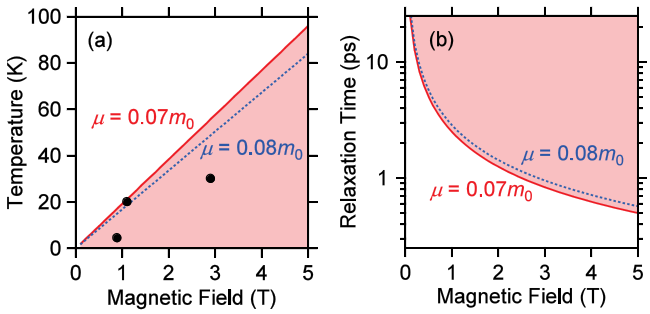

FIG. 4. Calculated magnetic-field dependencies of (a) the upper limit of the temperature and (b) lower limit of the carrier relaxation time for observing the Landau levels. The solid and dotted lines are results for the exciton reduced masses of $0.07m_0$ and $0.08m_0$, respectively. The shaded areas satisfy the criteria of $\hbar\omega_c > k_B T$ and $\omega_c\tau > 1$ for the exciton reduced mass of $0.07m_0$. The closed circles in (a) represent the experimental results shown in Figs. 3(d)–3(f).

limit of the carrier relaxation time for observing the Landau shift can be estimated using the obtained effective masses. Figures 4(a) and 4(b) show the calculated magnetic-field dependencies of the upper limit of the temperature and the lower limit of the carrier relaxation time, respectively. The solid and dotted lines are results for the exciton reduced mass of $0.07m_0$ and $0.08m_0$, respectively. The shaded areas in Fig. 4 satisfy the criteria of $\hbar\omega_c > k_B T$ and $\omega_c\tau > 1$ for the exciton reduced mass of $0.07m_0$. The closed circles in Fig. 4(a) represent the experimental results shown in Figs. 3(d)–3(f), where the critical magnetic field was estimated by the intercept of the linear magnetic-field dependence of the PL-peak energy as depicted by the arrows. Here, the linear magnetic-field dependence of the PL-peak energy does not pass through the origin, as is known in the case in which the Coulomb interaction is taken into account owing to the coexistence of the exciton and Landau levels.[32] The experimental results satisfy the criterion of $\hbar\omega_c > k_B T$. The discrepancy from the calculated line is considered to originate from the localized levels, as discussed in Fig. 3, because the localized states induce an increase of the effective mass, which results in the decrease of the upper limit of the temperature as shown by the dotted line in Fig. 4(a). Since the Landau shift appears approximately 1 T below 20 K, as shown in Fig. 4(a), the carrier relaxation time in highly N δ-doped GaAs is estimated to be longer than 1 ps, as shown in Fig. 4(b). According to the effective mass of $0.07m_0$ and the relaxation time of 1 ps, the mobility is calculated to be approximately 20 000 $cm^2/V{\cdot}s$ when we ignore the scattering processes. This calculated high mobility indicates the possibility of highly N δ-doped GaAs forming an epitaxial atomic sheet.

In conclusion, we have succeeded in growing an epitaxial two-dimensional N atomic sheet in GaAs by using the site-controlled N δ-doping technique. We observed a change in the electronic states of N δ-doped GaAs from the isolated impurity centers to the delocalized impurity band at 1.49 eV with increasing N-doping density. The excitation-power-, temperature-, and magnetic-field-dependent PL spectra show the electron delocalization in highly N δ-doped GaAs. The emission related to localized levels below the impurity band edge was dominant at low excitation power and temperature, whereas the effects of the localized levels can be neglected with increasing excitation power and temperature. With an effective mass of $0.07m_0$ and relaxation time of 1 ps estimated using the Landau shift, the mobility is calculated to be approximately 20 000 $cm^2/V{\cdot}s$ when we ignore the scattering processes. These observations indicate the formation of the epitaxial two-dimensional N sheet in GaAs.

This work was partially supported by a Grant-in-Aid for Scientific Research (No. 25630126) from the Ministry of Education, Culture, Sports, Science and Technology, Japan.

[1]K. S. Novoselov, A. K. Geim, S. V. Morozov, D. Jiang, M. I. Katsnelson, I. V. Grigorieva, S. V. Dubonos, and A. A. Firsov, Nature **438**, 197 (2005).
[2]Y. Zhang, Y.-W. Tan, H. L. Stormer, and P. Kim, Nature **438**, 201 (2005).
[3]B. Lalmi, H. Oughaddou, H. Enriquez, A. Kara, S. Vizzini, B. Ealet, and B. Aufray, Appl. Phys. Lett. **97**, 223109 (2010).
[4]P. Vogt, P. D. Padova, C. Quaresima, J. Avila, E. Frantzeskakis, M. C. Asensio, A. Resta, B. Ealet, and G. L. Lay, Phys. Rev. Lett. **108**, 155501 (2012).
[5]E. Bianco, S. Butler, S. Jiang, O. D. Restrepo, W. Windl, and J. E. Goldberger, ACS Nano **7**, 4414 (2013).
[6]K. S. Novoselov, A. K. Geim, S. V. Morozov, D. Jiang, Y. Zhang, S. V. Dubonos, I. V. Grigorieva, and A. A. Firsov, Science **306**, 666 (2004).
[7]A. H. C. Neto, F. Guinea, N. M. R. Peres, K. S. Novoselov, and A. K. Geim, Rev. Mod. Phys. **81**, 109 (2009).
[8]D. C. Elias, R. V. Gorbachev, A. S. Mayorov, S. V. Morozov, A. A. Zhukov, P. Blake, L. A. Ponomarenko, I. V. Grigorieva, K. S. Novoselov, F. Guinea, and A. K. Geim, Nature Phys. **7**, 701 (2011).
[9]S. V. Morozov, K. S. Novoselov, M. I. Katsnelson, F. Schedin, D. C. Elias, J. A. Jaszczak, and A. K. Geim, Phys. Rev. Lett. **100**, 016602 (2008).
[10]T. Ohta, A. Bostwick, T. Seyller, K. Horn, and E. Rotenberg, Science **313**, 951 (2006).
[11]M. Y. Han, B. Özyilmaz, Y. Zhang, and P. Kim, Phys. Rev. Lett. **98**, 206805 (2007).
[12]J. Bai, X. Zhong, S. Jiang, Y. Huang, and X. Duan, Nat. Nanotechnol. **5**, 190 (2010).
[13]R. Sako, N. Hasegawa, H. Tsuchiya, and M. Ogawa, J. Appl. Phys. **113**, 143702 (2013).
[14]B. Obradovic, R. Kotlyar, F. Heinz, P. Matagne, T. Rakshit, M. D. Giles, M. A. Stettler, and D. E. Nikonov, Appl. Phys. Lett. **88**, 142102 (2006).
[15]R. Hanson and D. D. Awschalom, Nature **453**, 1043 (2008).
[16]P. M. Koenraad and M. E. Flatté, Nature Mater. **10**, 91 (2011).
[17]T. Kita and O. Wada, Phys. Rev. B **74**, 035213 (2006).
[18]T. Kita, Y. Harada, and O. Wada, Phys. Rev. B **77**, 193102 (2008).
[19]Y. Harada, T. Kubo, T. Inoue, O. Kojima, and T. Kita, J. Appl. Phys. **110**, 083522 (2011).
[20]Y. Harada, O. Kojima, T. Kita, and O. Wada, Phys. Status Solidi B **248**, 464 (2011).
[21]T. Makimoto, H. Saito, and N. Kobayashi, Jpn. J. Appl. Phys., Part 1 **36**, 1694 (1997).
[22]D. G. Thomas and J. J. Hopfield, Phys. Rev. **150**, 680 (1966).
[23]M. Latkowska, R. Kudrawiec, G. Sęk, J. Misiewicz, J. Ibáñez, M. Henini, and M. Hopkinson, Appl. Phys. Lett. **98**, 131903 (2011).
[24]M. Baranowski, M. Latkowska, R. Kudrawiec, and J. Misiewicz, J. Phys.: Condens. Matter **23**, 205804 (2011).
[25]S. Shirakata, M. Kondow, and T. Kitatani, Appl. Phys. Lett. **80**, 2087 (2002).
[26]M. Elborg, M. Jo, Y. Ding, T. Noda, T. Mano, and K. Sakoda, Jpn. J. Appl. Phys., Part 1 **51**, 06FF15 (2012).
[27]Y. Harada, O. Kojima, T. Kita, and O. Wada, Phys. Status Solidi C **8**, 365 (2011).
[28]L. Viña, S. Logothetidis, and M. Cardona, Phys. Rev. B **30**, 1979 (1984).
[29]K. P. O'Donnell and X. Chen, Appl. Phys. Lett. **58**, 2924 (1991).
[30]S. Adachi, *Properties of Group-IV, III-V and II-VI Semiconductors*, 1st ed. (Wiley, Chichester, 2005).
[31]A. Polimeni, F. Masia, A. Vinattieri, G. B. H. von Högersthal, and M. Capizzi, Appl. Phys. Lett. **84**, 2295 (2004).
[32]O. Akimoto and H. Hasegawa, J. Phys. Soc. Jpn. **22**, 181 (1967).